A study of the nitrogen inversion barrier in quisqualic acid and its analogues

Cristina I. De Matteis and David E. Jackson
Department of Pharmaceutical Sciences, University of Nottingham, University Park, Nottingham, UK NG7 2RD

The geometry and inversion barrier of the ring substituted nitrogen in a quisqualic acid model compound 5, and the corresponding carbon (hydantoin) and nitrogen (dioxotriazolidine) analogues (6 and 7) has been investigated using the three MOPAC hamiltonians, PM3, AM1 and MNDO. In the case of the quisqualic acid and the nitrogen analogue model compounds, all three methods predict essentially pyramidal nitrogen configurations in agreement with X-ray crystallographic data for related compounds (1 and 8, respectively). For the carbon analogue model compound (6), only MNDO predicts a planar nitrogen geometry, in agreement with that found in the crystal structure of 3-(2,4-dioxo-2,3,4,5-tetrahydroimidazol-1-yl)alanine 3, with the other two methods suggesting a considerably more pyramidal structure. A search of the Cambridge crystallographic database indicates that nitrogen planarity is a general feature of this carbon containing hydantoin ring system, further emphasising the value of the MNDO hamiltonian when studying this type of heterocyclic structure. Our results indicate that different potential energy surfaces may be obtained from identical reaction coordinate calculations on different computer platforms, when PRECISE convergence criteria are used.

Introduction

L-Glutamic acid is an important excitatory neurotransmitter in both vertebrate and invertebrate systems, and it is generally thought that there are at least three main sites of action; namely quisqualate, kainate and N-methyl-D-aspartate responsive sites.[1] At quisqualate sensitive receptors, L-quisqualic acid (1),† a naturally occurring amino acid, is often more active than the endogenous L-glutamic acid (2).[2-4] We have recently reported a number of studies aimed at further understanding this potency difference and at probing the structure–activity relationships at this quisqualate sensitive site.

A method for the synthesis of quisqualic acid, together with its carbon (3) and nitrogen (4) analogues has recently been reported.[5] Patch clamp studies at the neuromuscular junction of the locust leg, a well defined quisqualate sensitive glutamatergic synapse, indicated that L-quisqualic acid was, as suggested from previous work, more active than L-glutamic acid. The carbon and nitrogen analogues showed no activity in this system.[6]

Recently reported results from X-ray crystallographic analysis of DL-quisqualic acid and the carbon analogue provided very interesting results and a possible explanation for the structure–activity data.[7] Quisqualic acid and the carbon analogue showed a striking difference in the geometry of the nitrogen atoms joining the heterocyclic ring to the amino acid side chain, with the nitrogen configuration in the latter almost planar, as would be expected in an amide group, whilst the configuration in quisqualic acid was essentially pyramidal. Additionally, racemic quisqualic acid showed the presence of both invertomers at the substituted ring nitrogen, the two enantiomers exhibiting opposite nitrogen configurations. Interestingly, the nitrogen configuration for L-quisqualic acid from this racemic crystal was opposite to that reported in the structure of the naturally occurring compound.[8] This suggests that the nitrogen invertomers in quisqualic acid are of comparable stability with the energy barrier for interconversion small. The above structural data indicates that activity at the quisqualate sensitive receptor may be related to a pyramidal

† Quisquatic acid = 3-(3,5-dioxo-1,2,4-oxadiazolidin-2-yl)alanine.

geometry at the substituted ring nitrogen. This would mimic the geometry of glutamic acid, where C-4, which is in an equivalent position to the ring substituted nitrogen in quisqualic acid, is sp³ hybridized.

The configuration of the substituted ring nitrogen and the barrier to inversion at this centre are clearly fundamental to an understanding of the structure–activity profile of these compounds at the quisqualate sensitive receptor. We have carried out preliminary semi-empirical molecular orbital calculations using MNDO on methyl substituted model structures 5–7.[7] In the case of compounds 5 and 6 the preferred configuration of the ring substituted nitrogens predicted from these calculations is in agreement with the X-ray crystallographic structures and for the quisqualate analogue (5) the predicted energy barriers for inversion at this nitrogen are such as to suggest rapid inversion at room temperature. For the nitrogen model compound 7, the preferred geometry of the ring substituted nitrogen is essentially pyramidal. Whilst no X-ray crystallographic data is available for either compounds 4 or 7, this data is available for the dioxotriazolidine 8, where both of the adjacent ring nitrogens are pyramidal.[9]

Given the reported inaccuracies of MNDO,[10] we report here a more detailed semi-empirical molecular orbital study of nitrogen inversion barriers in these molecules. Additionally, other examples of compounds containing the quisqualic acid and carbon analogue heterocyclic structures, derived from the Cambridge Crystallographic database,[11] are presented, and their structures compared with the quisqualic acid analogues.

Methods and results

Semi-empirical molecular orbital calculations
The methyl substituted model compounds 5–7 were studied, and the barrier to inversion for the ring substituted nitrogens was calculated using the three MOPAC hamiltonians, PM3, AM1 and MNDO.

The model compounds were constructed using the 2D sketch facilities in COSMIC.[12,13] All nitrogens were originally assigned trigonal planar atom types, charges were added with

1

2

5   X = O

3   X = CH$_2$

4   X = NH

6   X = CH$_2$

7   X = NH

8

9

10
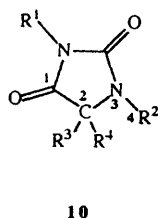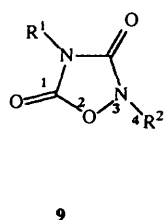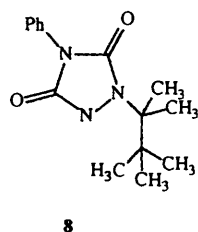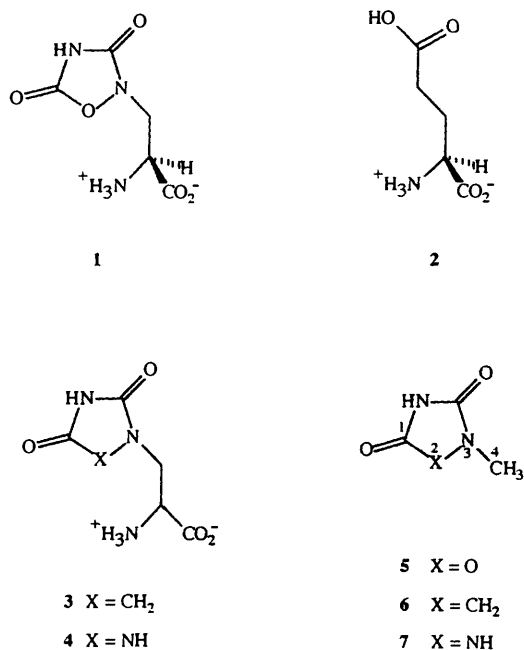
either the LIVERPOOL method[14] (carbon analogue) or CNDO (oxygen and nitrogen analogue),[15] and the resulting structures minimized within the COSMIC forcefield. These structures were used as the starting geometries for all subsequent MOPAC calculations.

In order to probe the preferred configuration of the ring substituted nitrogen and investigate the barrier to its inversion, dihedral angle 1–2–3–4 (which defines the ring nitrogen configuration) was swept from 100° to −100° in 10° increments, using the reaction coordinate option within MOPAC. At each point on the reaction coordinate the dihedral angle was constrained, whilst full geometry optimization was carried out. The initial point on all reaction coordinate runs was optimization of the input structure, with dihedral angle 1–2–3–4 constrained at its initial value. For example, for compound 6 the initial conformer had dihedral angle 1–2–3–4 constrained at −179.7°, the second conformer had the angle set at 100°, the third set at 110° and so on. All calculations were repeated with the three MOPAC hamiltonians, PM3, AM1 and MNDO, and were carried out with and without molecular mechanics treatment of amide bonds, to monitor the effect of this

procedure. As recommended by Boyd,[16] all calculations were carried out using the enhanced SCF and geometry convergence criteria defined by the key word PRECISE. All calculations were carried out on the APOLLO DN 10000 using MOPAC version 5.0.[17] As will be discussed later, significant differences in the energy profiles from these reaction coordinate runs were obtained depending on how the dihedral angle was altered and depending on the computer platform used.

The resulting energy profiles are shown in Fig. 1, and the values for dihedral angle 1–2–3–4 of the minimum energy structures, together with the barriers to inversion are shown in Table 1. During these reaction coordinate runs a variety of geometry optimization criteria were met. These included Herbert's test and Peter's test, and on many occasions although the gradient test was not satisfied, optimization was stopped because the heat of formation dropped by less than 0.003 kcal mol^{-1} after three iterations.‡ On three occasions the geometry optimization terminated because the line minimization failed twice in a row.

For both oxygen and carbon analogues (5 and 6) there is little difference in the shape of the energy profiles, the dihedral angle of the minimum energy structures or the barriers to inversion when molecular mechanics treatment of amide bonds is or is not used. There is some difference in the shape of the energy profiles for the nitrogen analogue, but no difference in the dihedral angle of the minimum energy structures. Two conformers, which are noted in Fig. 1, have clearly been incompletely optimized and these points were therefore not considered in the calculation of energy barriers. These structures aside, the use of molecular mechanics treatment or not produces, at most, a difference in the dihedral angle of the minimum energy structures of ± 10° and a difference in the energy barriers to inversion of 0.4 kcal mol^{-1}.

There is good agreement between the MNDO results for all three model compounds and the results published previously.[7] The shape of the energy profiles is very similar, with the position of minimum energy structures the same and barriers to inversion within approximately 0.3 kcal mol^{-1}.

For the quisqualic acid model compound (5), the potential energy profiles obtained with all three hamiltonians show two minimum energy structures at either ± 140° or ± 130°. This corresponds to an essentially pyramidal geometry for the ring substituted nitrogen, and additionally both invertomers are of comparable energy. The dihedral angles for the minimum energy structures show good agreement with those obtained from X-ray crystallography [+ 144° (ref. 8), ± 137° (ref. 7)]. The barrier to inversion varies with the hamiltonian used, the largest occurring with AM1, but all are sufficiently small to suggest rapid inversion at room temperature.

For the carbon analogue the potential energy profiles obtained from both AM1 and PM3 show minimum energy structures at ± 150° or − 140°, corresponding to an essentially pyramidal ring nitrogen geometry. Both invertomers are of the same energy and barriers to inversion small, suggesting rapid interconversion at room temperature. With MNDO, minimum energy structures are obtained at ± 170°, suggesting that a near planar nitrogen geometry will be most stable, with an extremely small barrier to inversion. In this case the nitrogen geometry predicted from the MNDO calculations is in closest agreement with that determined experimentally (+ 168°).[7]

For the nitrogen analogue all three hamiltonians produce potential energy curves which are very different in shape to the other two molecules. This has been noted previously, and the following explanation given.[7] Assuming both of the adjacent ring nitrogens have pyramidal configurations, then the
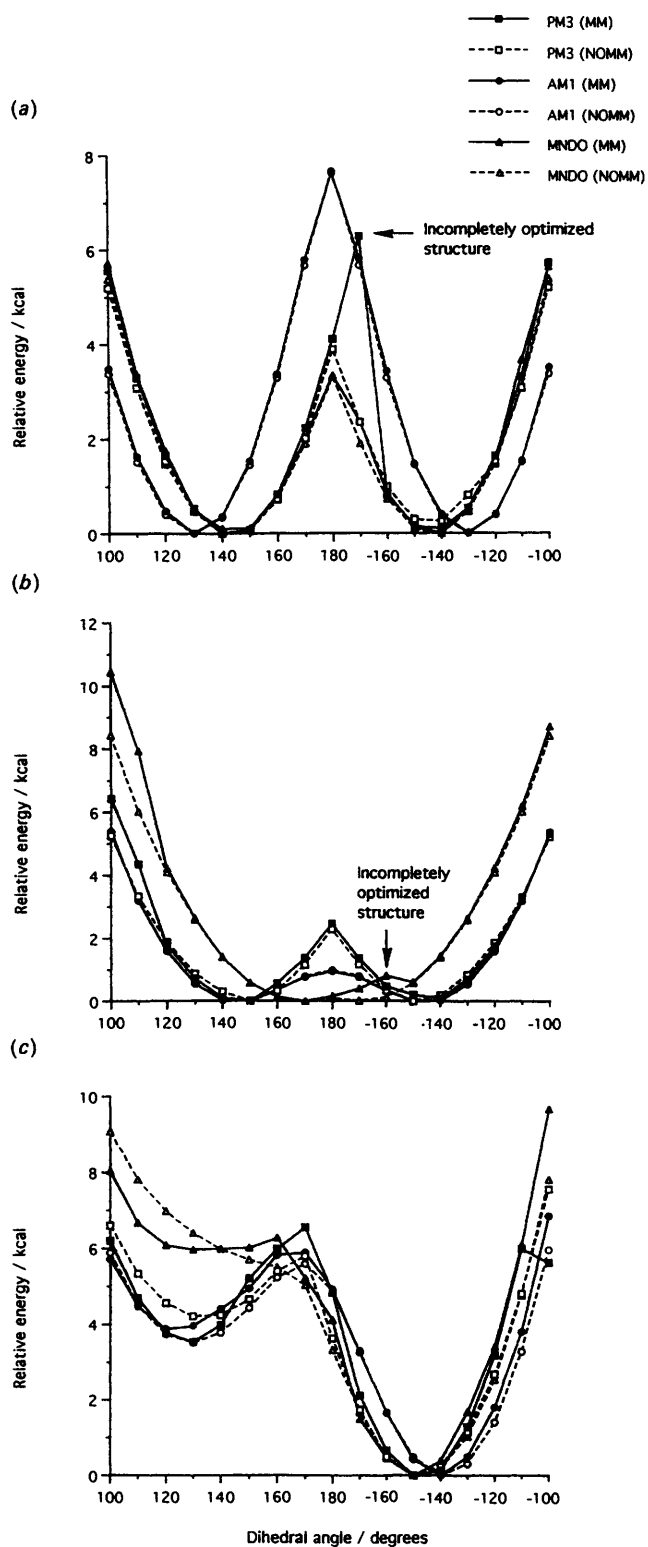
‡ 1 cal = 4.184 J.

Fig. 1 Relative energy profiles for (a) oxygen analogue 5, (b) carbon analogue 6, and (c) nitrogen analogue 7, with respect to dihedral angle 1-2-3-4, obtained with (MM) and without (NOMM) molecular mechanics treatment of amide bonds
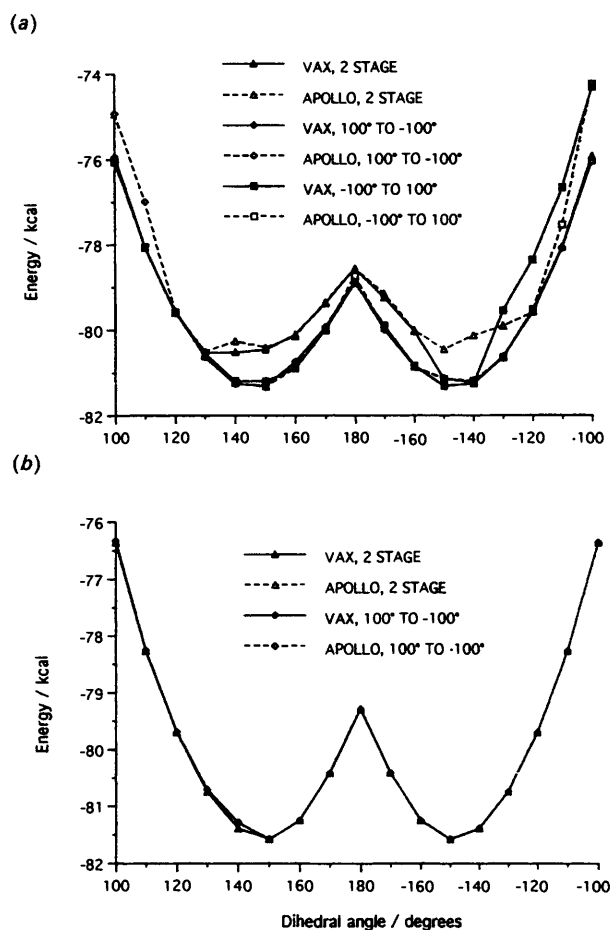

Fig. 2 Energy profiles obtained for carbon analogue 6 with PM3, including (a) and not including (b) molecular mechanics treatment of amide bonds, when the direction of the dihedral angle drive and the platform is altered

minimum energy structure corresponds to minimal lone pair interactions between the two nitrogen atoms, i.e. with the lone pairs positioned *trans*. All three hamiltonians predict pyramidal nitrogen geometry to be of lowest energy, with the corresponding dihedral angle agreeing with the experimentally determined geometry to within less than ± 6°.

Effect of platform and direction of dihedral angle drive on results

We have found considerable differences in the potential energy surfaces obtained depending on the direction the dihedral angle is altered and depending on the computer platform used. For studies on the carbon model compound with PM3, the energy profiles shown in Fig. 2 (including and not including molecular mechanics treatment of amide bonds) were obtained. Identical geometrical data was used as input for all the calculations (obtained as described in the section above) and PRECISE SCF and geometry optimization criteria were used on all occasions. All calculations were carried out on an APOLLO DN10000 and on a Micro-VAX II, and the following three dihedral angle driving routines were used: (a) 100° to − 100°, as described above; (b) − 100° to 100°; (c) two stage method: 180° to − 100° and 180° to 100°.

In agreement with the method described previously, the initial point on all reaction coordinate runs was optimization of the input structure with dihedral angle 1-2-3-4 constrained at its initial value. This was − 179.7° in all cases. Differences in the inversion barrier energy obtained depending on the conditions used are presented in Table 2.

Considerable differences in the shape of the potential energy surfaces and in the inversion barrier energies can be seen when the platform or dihedral angle driving routine is altered, for those calculations including a molecular mechanics treatment of the amide bonds. When this treatment is not included differences between runs are not significant; differences in inversion barrier energies are reflected at most in the fourth

Table 1 Nitrogen geometry (dihedral angle 1–2–3–4) in minimum energy structures and associated inversion energy barriers, and corresponding geometry from X-ray crystallographic studies

MOPAC Hamiltonian	Dihedral angle (1–2–3–4) in minimum energy structures	Barrier to inversion/kcal	Corresponding dihedral angle from X-ray crystallography
Compound 5			
PM3	+140°, −140° (MM)	4.11, 4.02	+144°,[a] ±137°[b]
	+140°, −140° (NOMM)	3.89, 3.63	
AM1	+130°, −130° (MM)	7.63, 7.62	
	+130°, −130° (NOMM)	7.66	
MNDO	+140°, −140° (MM)	3.24, 3.33	
	+140°, −140° (NOMM)	3.31	
Compound 6			
PM3	+150°, −140° (MM)	2.47, 2.38	+168°[c]
	+150°, −150° (NOMM)	2.29	
AM1	+150°, −150° (MM)	0.92, 0.94	
	+150°, −150° (NOMM)	0.99	
MNDO	+170° (MM)	0.15	
	+170°, −170° (NOMM)	0.08	
Compound 7			
PM3	−150° (MM)		+146°[d]
	−150° (NOMM)		
AM1	−140° (MM)		
	−140° (NOMM)		
MNDO	−150° (MM)		
	−150° (NOMM)		

[a] L-Quisqualic acid.[8] [b] DL-Quisqualic acid.[7] [c] One of the enantiomers selectively crystallized from the racemate.[7] [d] Compound 8.[9]

Table 2 Differences in inversion barrier energy for compound 6, when the direction of dihedral angle drive and the platform used is altered

Molecular mechanics treatment of amide bonds	Dihedral angle driving routine	Platform	Difference in inversion barrier energy/kcal[a]
Yes	a	VAX vs. APOLLO	0.04, 0.06
Yes	b	VAX vs. APOLLO	0.29, 0.04
Yes	c	VAX vs. APOLLO	0.04, 0.78
Yes	a vs. b	VAX	0.13, 0.03
Yes	a vs. b	APOLLO	0.12, 0.07
Yes	c vs. a	VAX	0.45, 0.23
Yes	c vs. b	VAX	0.31, 0.26
Yes	c vs. a	APOLLO	0.53, 0.49
Yes	c vs. b	APOLLO	0.65, 0.56
No	c	VAX vs. APOLLO	0, 0
No	a	VAX vs. APOLLO	0, 0
No	c vs. a	VAX	0, 0
No	c vs. a	APOLLO	0, 0

(a) 100° to −100°
(b) −100° to 100°
(c) Two-stage method: 180° to 100° and 180° to −100°

[a] Inversion barrier was calculated as the difference in energy between the appropriate minimum and maximum energy structures.

decimal place of kcal measurements. When this treatment is included, differences in inversion barrier energies vary from 0.03 to 0.78 kcal.

Differences in potential energy surfaces might be expected for calculations using alternative dihedral angle driving routines, as slightly different areas of conformational space will be entered and probed. Differences in results obtained between identical calculations run on different platforms has been documented elsewhere,[16] and has been attributed to differences in the numerical accuracy of various computers. In these cases the use of PRECISE convergence criteria appeared to remove these differences in calculated results. On both the APOLLO DN10000 and Micro-VAX II, floating point operations were carried out in double precision (64-bit words), the APOLLO using a 52 bit mantissa, and the Micro-VAX a 55 bit mantissa. The numerical accuracy of these two platforms is therefore slightly different, but in this work the use of PRECISE convergence criteria does not remove differences in calculated results. Although these differences in energy are, in general, not very large, the observation of discrepancies is noteworthy and worrying.

The largest differences in potential energy surfaces obtained for identical calculations on the two platforms were obtained with the two-stage dihedral angle driving protocol (Fig. 3). Considering the potential energy surface between −150° and −130°, where the largest differences were observed, the following was noted: on all occasions the Apollo conformers are of higher energy than the corresponding VAX structures. Analysis of the geometry optimization for these structures indicated that for the Apollo structure at −130° Herbert's test was satisfied, for the Apollo structure at −140° geometry optimization terminated because the line minimization failed twice in a row, and in the four remaining cases the gradient test was not satisfied but the optimization was stopped since the heat of formation dropped less than 0.003 kcal mol⁻¹ after three iterations.
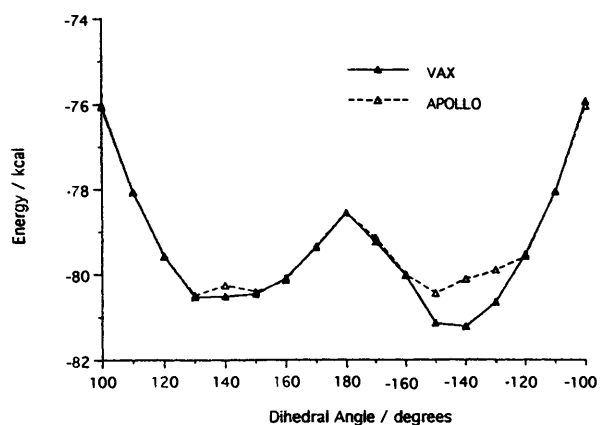
Fig. 3 Energy profiles obtained for carbon analogue 6 on the APOLLO and VAX using PM3, with molecular mechanics treatment of amide bonds (MM) and the two-stage dihedral angle drive

Fig. 4 Alteration in energy profile with complete minimization on original or alternative platform

All of these six structures were submitted for further minimization, on both the original and alternative platform, with minimization repeated until Herbert's test was satisfied. In other words the structure produced from a given unsuccessful minimization was re-submitted for further optimization. In all cases dihedral angle 1-2-3-4 was constrained as described above, whilst full geometry optimization allowed. In three cases repeated minimization (three or four attempts) produced no change in energy, and reported that geometry optimization had been terminated because the line minimization failed twice in a row. In all other cases Herbert's test was satisfied after between 1 and 16 attempts. The original and optimized potential energy surfaces are shown in Fig. 4, where those re-optimized structures not satisfying Herbert's test are indicated.

All minimizations produced lower energy structures than from the initial dihedral angle driving calculations, although this drop in energy varied considerably. Interestingly, the only original structure to satisfy Herbert's test also dropped in energy (by 0.7 kcal) when minimized on both platforms, requiring three further minimization attempts before satisfying Herbert's test again. The number of minimization attempts required before Herbert's test was satisfied varied from between one and nine on the VAX, and between one and 16 on the Apollo.

Considering the structures at −150°, the structures originating from the Apollo remain at approximately 0.7 kcal higher energy on minimization than the VAX originating structures. This suggests that different potential energy surfaces are being probed on the two platforms. The Apollo originating structures at −140° drop considerably in energy when minimized on both platforms, but to different energies depending on the platform. Minimization on the Apollo produces a conformer of very similar energy to the VAX originating structures (slightly lower in energy than the VAX conformers), whilst minimization on the VAX produces a structure 0.3367 kcal higher in energy than the Apollo minimized structure. This latter structure does not satisfy Herbert's rule, but complete geometry optimization cannot be achieved. The structures at −130° resulting from minimization are essentially of the same energy irrespective of platform.

These results suggest that in most cases the original differences in potential energy surface result from incomplete minimization. However, in three cases these differences do not disappear. Complete minimization of the Apollo structure at −150° on the Apollo produces a minimum energy structure approximately 0.7 kcal higher in energy than the other fully minimized structures. It would appear that the dihedral angle
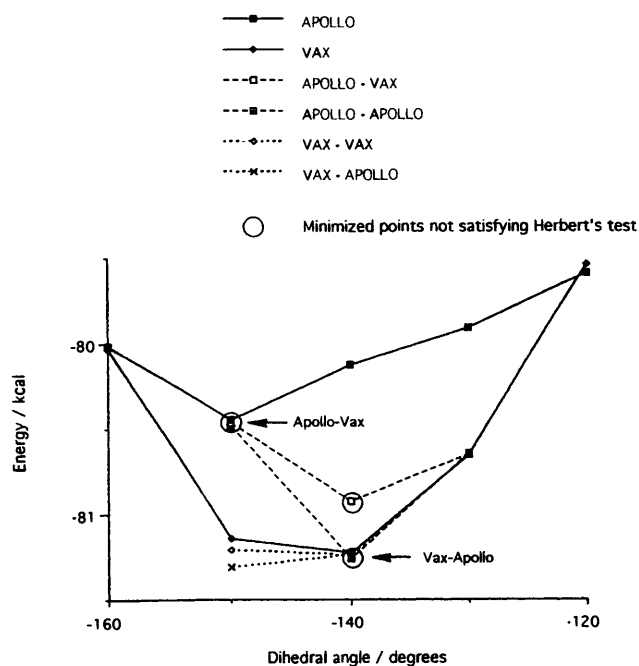
runs on different platforms have strayed down slightly different potential energy surfaces. The other two points which remain at higher potential energy than equivalent minimized structures do not satisfy Herbert's test. This may explain why the potential energy surfaces differ, but also illustrates the inadequacy of this minimizer, since the true minimum cannot be located.

Calculated nitrogen inversion barriers in ammonia and methylamine

Nitrogen inversion barriers in ammonia and methylamine were calculated using AM1, PM3 and MNDO. Structures were constructed using the 2D sketch facilities in COSMIC, charges were added using the LIVERPOOL method and structures initially minimized within the COSMIC forcefield. In each case two sets of structures were generated, one with a trigonal planar nitrogen atom type, the other with a pyramidal Nsp^3 atom type. These structures were used as starting geometries for all subsequent MOPAC calculations.

The inversion barrier energy was calculated as the difference in energy between the molecule with planar and pyramidal nitrogen geometry. The pyramidal geometry was obtained by unrestrained geometry optimization, whilst the planar geometry required the use of constraints during minimization. For ammonia two HNH angles were constrained at 120°, whilst for methylamine, the H(H)NC improper dihedral angle was constrained at 180° and a CNH angle constrained at 120°. PRECISE convergence criteria were used, and minimization continued until Peter's test was satisfied. Calculations were carried out on the VAX. Results are given in Table 3. Visualization of the minimized methylamine structures indicated that in all cases for the planar structure, one N–H bond showed an eclipsed arrangement with respect to a C–H bond. An alternative planar input structure was generated from the COSMIC sketch facilities, with the H–C–N–H dihedral angle altered to 30°. This structure produced lower energy minima from MOPAC geometry optimization, and on visualization showed a staggered arrangement between these bonds. These energy values were used to calculate the inversion barrier.

The results obtained for ammonia are in exact agreement

with those reported by Stewart.[10] Comparing calculated inversion barriers with experimental values, indicates that AM1 provides the best agreement. PM3 is superior to MNDO when considering ammonia, whilst the reverse is true in the case of methylamine.

Crystallographic data

A search of the Cambridge crystallographic database[11] for structures of the type 9 and 10 provided those shown in Table 4. Only those structures in which R^2 is a substituent with carbon directly bonded to the ring nitrogen are included. Structures in which R^2 = H were not considered because of the difficulties in locating the position of hydrogen atoms by X-ray crystallography. The value for dihedral angle 1–2–3–4 is provided.

For structure 9 only two analogues were located, quisqualic acid[8] and the equivalent structure where R^2 = H,[19] where the dihedral angle 1–2–3–4 is equal to $-144.54°$ and $-179.38°$, respectively. In the latter example, the authors state that the position of the hydrogen atom at R^2 'was fixed from stereochemical considerations and was not included either in structure factor calculations or in the least squares refinement'. This result does not therefore stem from experimental observation, and as such can be ignored within the context of this study. For structure 10 a number of compounds were located, and in each case the dihedral angle 1–2–3–4 is equal to $180 (\pm 10)°$.

Discussion

All of the hamiltonians used in this work predict the quisqualic acid model compound to have a pyramidal ring substituted

Table 3 Calculated and experimentally determined nitrogen inversion barriers (kcal mol⁻¹)
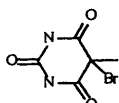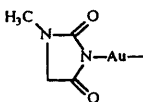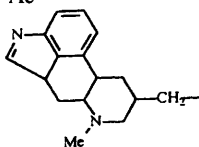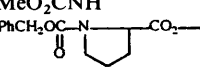
	PM3	AM1	MNDO	Experimental
Ammonia	9.98	4.24	11.58	5.8[10]
Methylamine	9.08	4.20	7.66	4.8[18]

nitrogen, in agreement with X-ray crystallographic data for quisqualic acid, with both invertomers of comparable stability, and the barrier to nitrogen inversion sufficiently small to allow rapid inversion at room temperature. Similarly, all the hamiltonians predict the nitrogen analogue to have a pyramidal nitrogen configuration. Further support for compounds 4 and 7 possessing a pyramidal ring substituted nitrogen comes from the X-ray crsytallographic data for the structurally similar compound 8. In the case of the carbon analogue, MNDO predicts a near planar ring substituted nitrogen, which agrees with X-ray crystallographic data, whilst AM1 and PM3 suggest a pyramidal nitrogen geometry. It therefore appears that MNDO, which is the oldest of the three MOPAC hamiltonians used in this study, best reproduces the experimental geometry of the ring substituted nitrogen in the carbon analogue.

Our comparisons of inversion barrier energies calculated with MNDO, AM1 and PM3 for ammonia and methylamine, with experimental energy values, indicate that AM1 provides the best agreement, with PM3 proving superior to MNDO for ammonia and MNDO superior to PM3 for methylamine. We cannot comment on the relative accuracy of these three hamiltonians with compounds 5 and 7, since nitrogen geometry is correctly predicted in all cases and we have no quantitative experimental data for inversion barrier energies. However, for the carbon model compound 6, MNDO is clearly superior to both AM1 and PM3.

Obviously, inversion barrier energies will be dependent on the composition of the bulk phase and in particular solvent effects would be expected in solution. Energies derived from these calculations do not consider intermolecular effects, and should therefore be treated with some caution. In addition, the effect of crystal packing forces on molecular geometry should not be ignored. A study of nitrogen geometry in the crystal structures of a series of amine containing central nervous system drugs suggested that crystal packing forces are, in general, insufficient to have a major effect on nitrogen geometry.[29] Furthermore, the ring substituted nitrogen geometries predicted for model compounds 5 and 7 from our calculations are

Table 4 Nitrogen geometry (dihedral angle 1–2–3–4) for oxygen and carbon analogues (9, 10) located within the Cambridge crystallographic database

	R^1	R^2	R^3	R^4	Dihedral angle 1–2–3–4
Oxygen analogues (9)	H	$H_3N^+C(CO_2^-)HCH_2$			$-144.54°$[8]
Carbon analogues (10)		Me	H	H	$+173.63°$[20]
		Me	H	H	$\pm178.49°$, $\pm174.49°$[21]
	Ac	Me	Me	Me	$-174.91°$[22]
	H	$C_6H_{11}CHOH[CH_2]_2$	H	$^-O_2C[CH_2]_6$	$-176.18°$[23]
	p-ClC₆H₄	p-ClC₆H₄NHCO	H	$(CH_3)_2NCO$	$-172.37°$[24]
	PhCH₂	Ac	H	MeO₂CCH₂	$+170.46°$[25]
	H		H	H	$+178.39°$[26]
	p-MeC₆H₄	PhCO	Ph	MeO₂CNH	$-170.84°$[27]
	H	Me	H		$+175.22°$[28]

in agreement with X-ray crystallographic structures, again suggesting a limited crystal packing effect on nitrogen geometry. In the case of model compound **6**, where an essentially planar ring appears to be a general feature in the crystal structures of molecules with this heterocyclic system, there is agreement between the geometry calculated from MNDO and the X-ray crystallographic structure.

In these complicated five-membered ring systems, nitrogen geometry will be dependent on subtle electronic and steric factors. A survey of nitrogen geometry in a series of amine containing central nervous system drugs, derived from the Cambridge crystallographic database, showed that configuration varied continuously between typical sp^3 and typical sp^2, and that, in general, the presence of an adjacent carbonyl group favoured planarity. Additionally, the presence of nitrogen within a five membered ring system did not appear to affect the nitrogen geometry.[29] It has been reported that an electronegative atom α to nitrogen will slow down the rate of inversion and favour sp^3 hybridization.[30] It therefore appears that in quisqualic acid this latter effect is stronger than the tendency for the nitrogen to assume sp^2 planar geometry, in which case conjugation in the ring between the adjacent amide groups would be expected.

All of the structures located in the Cambridge crystallographic database with the same heterocyclic structure as the carbon analogue, also possess an essentially planar ring substituted nitrogen, suggesting that this is a general feature of this structural unit. This further emphasizes the value of the MNDO hamiltonian when studying this type of heterocyclic system.

Finally our results indicate that depending on which computer platform calculations are carried out on, different potential energy surfaces may be obtained. These differences appear to reflect either poor minimization, so that upon complete minimization these differences disappear, or genuine differences in the potential energy surfaces which are explored by calculations on different computers. Differences in potential energy surfaces obtained from identical reaction coordinate runs, using MOPAC 3.1 and default settings (including the Davidon–Fletcher–Powell geometry optimization procedure), on different computers has previously been reported. The use of PRECISE settings for SCF convergence and geometry optimization criteria was reported to have essentially removed these differences (heats of formation values agreed to the first or second decimal place). These discrepancies were attributed to the different numerical accuracy of various computers, so that the geometry optimizer may move down different potential energy surfaces, if a number are available, of very similar energy.

Additionally, a note which was added in proof, suggests that the Broyden–Fletcher–Goldfarb–Shanno (BFGS) geometry optimizer, which is the default in later versions of MOPAC, is more robust to rounding errors in minimizations, but PRECISE settings are still needed.[16] Our work using MOPAC 5.0, with the BFGS geometry optimizer shows a reduction in differences between potential energy surfaces obtained from different computers when PRECISE is used, but significant differences remain, presumably arising from floating point rounding errors.

References

1 J. C. Watkins and R. H. Evans, *Annu. Rev. Pharmacol.*, 1981, **21**, 165.
2 S. G. Cull-Candy, R. Miledi and I. Parker, *J. Physiol.*, 1981, **321**, 195.
3 K. A. F. Gration, J. J. Lambert, R. L. Ramsey, R. P. Rand and P. N. R. Usherwood, *Brain Res.*, 1981, **230**, 400.
4 K. A. F. Gration and P. N. R. Usherwood, *Verh. Dtsch. Zool. Ges.*, 1980, 122.
5 B. W. Bycroft, S. R. Chhabra, R. J. Grout and P. J. Crowley, *J. Chem. Soc., Chem. Commun.*, 1984, 1156.
6 P. Boden, B. W. Bycroft, S. R. Chhabra, J. Chiplin, P. J. Crowley, R. J. Grout, T. J. King, E. McDonald, P. Rafferty and P. N. R. Usherwood, *Brain Res.*, 1986, **385**, 205.
7 D. E. Jackson, B. W. Bycroft and T. J. King, *J. Comput.-Aided Mol. Design*, 1988, **2**, 321.
8 J. L. Flippen and R. D. Gilardi, *Acta Crystallogr., Sect. B*, 1976, **32**, 951.
9 R. J. Baker, J. W. Timberlake, J. T. Alender, R. J. Majeste and L. M. Trefonas, *Cryst. Struct. Commun.*, 1982, **11**, 763.
10 J. J. P. Stewart, *J. Comput.-Aided Mol. Design*, 1990, **4**, 1.
11 F. H. Allen, J. E. Davies, J. J. Galloy, O, Johnson, O. Kennard, C. F. Macrae, E. M. Mitchell, G. F. Mitchell, J. M. Smith and D. G. Watson, *J. Chem. Inf. Comput. Sci.*, 1991, **31**, 187.
12 J. G. Vinter, A. Davis and M. R. Saunders, *J. Comput.-Aided Mol. Design*, 1987, **1**, 31.
13 S. D. Morley, R. J. Abraham, I. S. Haworth, D. E. Jackson, M. R. Saunders and J. G. Vinter, *J. Comput.-Aided Mol. Design*, 1991, **5**, 475.
14 R. J. Abraham, G. H. Grant, I. S. Haworth and P. E. Smith, *J. Comput.-Aided Mol. Design*, 1991, **5**, 21.
15 J. A. Pople and D. L. Beveridge, *Approximate Molecular Orbital Theory*, McGraw-Hill, New York, 1970.
16 D. B. Boyd, D. W. Smith, J. J. P. Stewart and E. Wimmer, *J. Comput. Chem.*, 1988, **9**, 387.
17 J. J. P. Stewart, *Quantum Chem. Prog. Exch. Bull.*, 1989, **9**, 10. QCPE Program 455, Version 5.0.
18 W. J. Hehre, L. Radom, P. V. R. Schleyer and J. A. Pople, *Ab initio molecular orbital theory*, Wiley, New York, 1986, p. 265.
19 A. S. Begum, V. K. Jain, S. Ramakumar and C. L. Khetrpal, *Acta Crystallogr., Sect. C*, 1988, **44**, 195.
20 C. Pascard-Billy, *Acta. Crystallogr., Sect. B*, 1970, **26**, 1418.
21 N. A. Malik, P. J. Sadler, S. Neidle and G. L. Taylor, *J. Chem. Soc., Chem. Commun.*, 1978, 711.
22 J. M. Andrieu, E. E. Castellano, A. G. Alvarez, J. Zinczuk, R. A. Corral and O. O. Orazi, *Rev. Latinoam. Quim.*, 1979, **10**, 14.
23 M. A. Brockwell, A. G. Caldwell, N. Whittaker and M. J. Begley, *J. Chem. Soc., Perkin Trans. 1*, 1981, 706.
24 E. Schaumann, S. Grabley and G. Adiwidjaja, *Justus Liebigs Ann. Chem.*, 1981, 264.
25 L. D. Keys III, K. Folting, W. E. Streib and M. Johnston, *J. Org. Chem.*, 1986, **51**, 4721.
26 E. Foresti, P. Sabatino, L. R. Di Sanseverino, R. Fusco, C. Tosi and R. Tonani, *Acta Crystallogr., Sect. B*, 1988, **44**, 307.
27 T. Sheradsky and N. Itzhak, *J. Chem. Soc., Perkin Trans. 1*, 1989, 33.
28 K. Ienaga, K. Nakamura, A. Ishii, T. Taga, Y. Miwa and F. Yoneda, *J. Chem. Soc., Perkin Trans. 1*, 1989, 1153.
29 P. R. Andrews, S. L. A. Munro, M. Sadek and M. G. Wong, *J. Chem. Soc., Perkin Trans. 2*, 1988, 711.
30 F. G. Riddell, *The Conformational Analysis of Heterocyclic Compounds*, Academic Press, London, 1980, p. 84.